

1           **THE QUORUM SENSING PEPTIDE ENTF\* PROMOTES COLORECTAL CANCER**

2           **METASTASIS IN MICE: A NEW FACTOR IN THE MICROBIOME-HOST INTERACTION**

3           Nathan Debuinne<sup>1,\*</sup>, Evelien Wynendaele<sup>1,\*</sup>, Yorick Janssens<sup>1</sup>, Anton De Spiegeleer<sup>1,2</sup>,  
4           Frederick Verbeke<sup>1</sup>, Liesa Tack<sup>1</sup>, Sophie Van Welden<sup>2</sup>, Evy Goossens<sup>3</sup>, Daniel Knappe<sup>4</sup>, Ralf  
5           Hoffmann<sup>4</sup>, Christophe Van De Wiele<sup>5</sup>, Debby Laukens<sup>2</sup>, Peter Van Eenoo<sup>5</sup>, Filip Van  
6           Immerseel<sup>3</sup>, Olivier De Wever<sup>6</sup> & Bart De Spiegeleer<sup>1</sup>

7

8           <sup>1</sup> Drug Quality and Registration Group, Faculty of Pharmaceutical Sciences, Ghent  
9           University, Ghent, Belgium. <sup>2</sup> Department of Internal Medicine and Pediatrics, Faculty of  
10          Medicine and Health Sciences, Ghent University, Ghent, Belgium. <sup>3</sup> Department of Pathology,  
11          Bacteriology and Poultry diseases, Faculty of Veterinary Medicine, Ghent University, Ghent,  
12          Belgium. <sup>4</sup> Center of Biotechnology and Biomedicine, Faculty of Chemistry and Mineralogy,  
13          Universität Leipzig, Leipzig, Germany. <sup>5</sup> Department of Diagnostic Sciences, Faculty of  
14          Medicine and Health Sciences, Ghent University, Ghent, Belgium. <sup>6</sup> Department of Human  
15          Structure and Repair, Faculty of Medicine and Health Sciences, Ghent University, Ghent,  
16          Belgium.

17          \* These authors contributed equally: Nathan Debuinne, Evelien Wynendaele.

18

19          Email: Nathan.Debuinne@UGent.be; ejwynend.Wynendaele@UGent.be; Yorick.Janssens@UGent.be;  
20          Anton.DeSpiegeleer@UGent.be; Frederick.Verbeke@UGent.be; Liesa.Tack@UGent.be;  
21          Sophie.VanWelden@UGent.be; Evy.Goossens@UGent.be; daniel.knappe@bbz.uni-leipzig.de;  
22          Ralf.hoffmann@bbz.uni-leipzig.de; Christophe.VandeWiele@UGent.be; Debby.laukens@ugent.be;  
23          Peter.Vaneenoo@ugent.be; Filip.Vanimmerseel@ugent.be; Olivier.Deweever@ugent.be;  
24          Bart.despiegeleer@ugent.be

25

26          **Corresponding author**

27          Bart De Spiegeleer, Drug Quality and Registration Group, Faculty of Pharmaceutical  
28          Sciences, Ghent University, Ottergemsesteenweg 460, B-9000 Ghent, Belgium. E-mail:  
29          [Bart.DeSpiegeleer@UGent.be](mailto:Bart.DeSpiegeleer@UGent.be). Phone: +32 9 264 81 00

30

31 **ABSTRACT**

32 **Background:** Colorectal cancer, one of the most common malignancies worldwide, is  
33 associated with a high mortality rate, mainly caused by metastasis. Comparative metagenome-  
34 wide analyses between healthy individuals and cancer patients suggest a role for the human  
35 intestinal microbiota. Nevertheless, which microbial molecules are involved in this  
36 communication is largely unknown, with current studies mainly focusing on short chain fatty  
37 acids and amino acid metabolites as potential mediators. However, quorum sensing peptides  
38 are not yet considered in this microbiome-host interaction: their *in vivo* presence nor any *in vivo*  
39 host-effect have been reported.

40 **Results:** For the first time, we showed that a quorum sensing peptide metabolite, EntF\*  
41 produced by intestinal microbiota (*E. faecium*), is present in the blood circulation of mice.  
42 Moreover, it significantly promotes colorectal cancer metastasis *in vivo*, with metastatic lesions  
43 found in both liver and lung tissues, using an orthotopic mice model evaluating  
44 bioluminescence as well as macroscopic and microscopic presence of metastatic tumour  
45 nodules. *In vitro* tests on E-cadherin expression levels thereby indicated that the first, second,  
46 sixth and tenth amino acid of EntF\* were critical for the epithelial-mesenchymal transition  
47 (EMT) effect, responsible for tumour metastasis.

48 **Conclusion:** This paper adds a new group of molecules, the quorum sensing peptides, as an  
49 additional causative factor explaining the microbiome-host interaction. The presence of a  
50 selected quorum sensing peptide (metabolite) in the mouse was proven for the first time and its  
51 *in vivo* effect on colorectal metastasis was demonstrated. We anticipate our *in vivo* results to be  
52 a starting point for broader microbiome-health investigations, not only limited to colorectal  
53 cancer metastasis, but also for developing novel bio-therapeutics in other disease areas, giving  
54 due attention to the QSP produced by the microbiome.

55 **KEYWORDS:** quorum sensing peptides; microbiota; colorectal cancer metastasis; orthotopic  
56 mice model; LC-MS.

57 **BACKGROUND**

58 Colorectal cancer (CRC) is the third most common malignancy worldwide and  
59 associated with a high mortality rate, mainly caused by metastasis (mCRC). Primary CRC  
60 originates from epithelial cells that line the gastrointestinal tract, usually (but not always)  
61 through an adenoma-carcinoma sequence in the CRC tumorigenesis<sup>1</sup>: normal colorectal  
62 epithelium transforms to an adenoma and ultimately to an invasive and metastatic tumour. In a  
63 first step of the metastasis process, the epithelial CRC cells switch towards a mesenchymal  
64 phenotype, known as epithelial-to-mesenchymal transition (EMT)<sup>2</sup>. Although a clear hereditary  
65 component in CRC tumorigenesis is present in some cases, a strong association with diet and  
66 lifestyle has been demonstrated as well<sup>3</sup>. Moreover, also inflammation is believed to play a role  
67 in CRC cancer development, as a driver, illustrated by colitis-associated colon (CAC) cancers  
68 in patients with inflammatory bowel diseases (IBD), as well as a consequence, seen in patients  
69 with sporadic colorectal cancer<sup>4</sup>.

70 Growing evidence obtained in the last decade also suggests a role for the human  
71 intestinal microbiota in CRC<sup>5-7</sup>. For example, by comparing faeces from healthy persons and  
72 patients, higher abundances of *Enterococcus*, *Escherichia* and *Fusobacterium* species were  
73 observed in multiple intestinal disorders, including colorectal cancer (CRC) and Crohn's  
74 disease<sup>8-11</sup>. However, the causative factors for disease development or progression are not well  
75 understood and current research is mainly limited to bacterial-derived short-chain fatty acids  
76 and amino acid-derived amines<sup>12</sup>.

77 Quorum sensing peptides are traditionally regarded as intra- and inter-bacterial  
78 communication molecules; however, given their wide structural variety and co-evolution, we  
79 anticipate that these bacterial metabolites may also interact with the host. Different quorum  
80 sensing peptides were indeed previously found to influence the behaviour of the host cells,  
81 going from cancer cells (colorectal and breast cancer) towards brain and muscle cells<sup>13-16</sup>. In  
82 colorectal cancer, specific microbial quorum sensing peptides were found to promote tumour

83 cell invasion and angiogenesis *in vitro*, indicating the possible pro-metastatic properties of these  
84 peptides. In this study, we focus on *Enterococcus faecium*, one of the most abundant species in  
85 the human intestinal microbiota, which synthesizes the enterocin induction factor, *i.e.* the  
86 propeptide of the EntF quorum sensing peptide (AGTKPQGKPASNLVECVFSLFKCN).  
87 This peptide serves as a communication signal, regulating the production of enterocin A and B  
88 toxins, which are produced to inhibit the growth of similar or closely related bacterial  
89 strains<sup>17-22</sup>.

90 Up till now, however, quorum sensing peptides have not yet been unambiguously  
91 demonstrated to be present in biofluids. Only an indirect indication of the *in vivo* presence of  
92 an unidentified quorum sensing peptide was described in the stool of patients suffering from a  
93 *Clostridium difficile* infection<sup>23</sup>. Indicating the biological presence of certain quorum sensing  
94 peptides in mice, together with their *in vivo* effect on the host, may stimulate the research  
95 towards the additional role of quorum sensing peptides in the microbiome-host interaction.

96

## 97 **RESULTS AND DISCUSSION**

### 98 ***Biological presence of EntF\* in mice***

99 *In vitro* metabolism studies of EntF (Fig. 1a) in faeces and colonic mice tissue  
100 homogenates quickly yielded a 15-mer peptide EntF\* (SNLVECVFSLFKCN) (Fig. 1b), with  
101 a mean ( $\pm$  s.e.m.) formation rate of  $1.71 (\pm 0.27)\% \text{ min}^{-1}$  and  $0.11 (\pm 0.01)\% \text{ min}^{-1}$ , respectively.  
102 Similar to other quorum sensing peptides<sup>14</sup>, this EntF\* peptide is also able to cross the intestinal  
103 barrier *in vitro*, using a CaCo-2 monolayer permeability assay, with a mean ( $\pm$  s.e.m.) apparent  
104 permeability coefficient of  $3.70 (\pm 0.22) \times 10^{-9} \text{ cm s}^{-1}$  (Fig. 1c). These *in vitro* studies thus  
105 indicated that EntF\* can be present in the blood circulation of the host, *i.e.* after degradation of  
106 the endogenously present EntF to EntF\* in the colon or faeces and subsequent intestinal  
107 absorption of the EntF\* peptide.

108

109 To unambiguously demonstrate the *in vivo* presence of EntF\*, a bioanalytical method  
110 using reversed phase ultra-high-performance liquid chromatography coupled to a triple  
111 quadrupole mass spectrometer (RP-UPLC-TQ-MS) in Multiple Reaction Monitoring (MRM)-  
112 mode was developed and optimized, aiming to avoid carry-over and adsorption, as well as to  
113 maximize the selectivity and sensitivity. Critical methodological aspects to achieve these goals  
114 were: (1) a suitable sample preparation method using a novel bovine serum albumin (BSA)-  
115 based anti-adsorption solution<sup>24</sup> and the combination of solvent/acid/heat sample treatment  
116 followed by solid phase extraction, and (2) appropriate MS detection settings, including the  
117 selection of quantifier ( $b_2$ :  $m/z= 202.08$ ) and qualifier ( $b_3$ :  $m/z= 315.17$ ) ions. The method was  
118 suitably verified and found to be appropriate for its purpose (Supplementary Fig. 1). Serum  
119 samples of 35 healthy, non-manipulated mice (C57BL/6 mice, aged 5-18 months) were  
120 collected and analysed for the endogenous, natural presence of EntF\* (Fig. 1d), using the  
121 developed RP-UPLC-TQ-MS (LC<sub>1</sub>-MS<sub>1</sub>) method. For six mice, the presence of EntF\* was  
122 observed in their serum above the limit of quantification (LOQ) of 100 pM (Fig. 1e). Taking  
123 into account all mice results, *i.e.* including the <LOQ (zero) values, an overall estimated mean  
124 value of 305 pM (s.e.m.=138 pM; n=35) was obtained (Supplementary Table 1). Following  
125 these findings, further evidence was obtained by subjecting a selected set of samples to three  
126 additional chromatographic methods: Hydrophilic Interaction Liquid Chromatography  
127 (HILIC)-UPLC-TQ-MS (LC<sub>2</sub>-MS<sub>1</sub>) (Fig. 1f) as an orthogonal separation system, and RP-  
128 UPLC-QTOF-MS (LC<sub>1</sub>-MS<sub>2</sub>) and RP-UPLC-QOrbitrap-MS (LC<sub>1</sub>-MS<sub>3</sub>) as high-resolution  
129 mass spectrometers. Serum samples of eight mice (four positive and four negative samples (*i.e.*  
130 above and below the LOQ, respectively, based on the RP-UPLC-TQ-MS findings)) were  
131 analysed using these additional methods (Fig. 1f-h). The presence and identity of EntF\* was  
132 confirmed using the isotopic distribution of the doubly charged precursor ion (Fig. 1g) and the

133 presence of fragment ions  $y_{11}$  ( $m/z= 1315.61$ ) and  $y_{12}$  ( $m/z= 1414.69$ ) (Fig. 1h) in the four  
134 positive serum samples (Supplementary Table 1). Finally, quantitative real-time PCR analysis  
135 on the associated faeces samples was performed to demonstrate the existence of EntF\*-  
136 containing *E. faecium* DNA copies (Supplementary Fig. 2, Supplementary Table 1): EntF\*  
137 DNA copies were indeed observed in all four positive samples. The faeces samples that  
138 contained the EntF\* gene but tested negative during the serum UPLC-MS analyses (e.g. sample  
139 20181011S8) could possess specific *E. faecium* strains that show a reduced translational  
140 efficiency. This is also observed in the data that are presented in Supplementary Table 2: out of  
141 the three *E. faecium* strains that contain the EntF gene, only one strain produced EntF *in vitro*  
142 (LoD = 1.5 nM). In addition, standard protein BLAST searches indicated no endogenous  
143 presence of the EntF\* peptide sequence in the murine genome (maximum sequence alignment  
144 of 67%), which is again a strong indication of the microbial origin of the *in vivo* found EntF\*  
145 peptide.

146

#### 147 ***In vitro activity and molecular target of EntF\****

148 EntF\* was previously found by our group to selectively promote angiogenesis and  
149 tumour cell invasion in screening *in vitro* experiments using HCT-8 colorectal cancer cells<sup>13,14</sup>.  
150 These *in vitro* effects were now confirmed and extended. Using Western blotting, EntF\* and  
151 some alanine- or D-amino acid derived analogues affected E-cadherin expression, which is  
152 linked to the epithelial-mesenchymal transition (EMT) of cancer cells (Fig. 2a, 2b and 2c,  
153 Supplementary Fig. 3). A mean significant decrease of 38% in E-cadherin expression was  
154 determined for EntF\*. When the first, second or tenth amino acid of EntF\* was replaced by an  
155 alanine amino acid, this decrease was significantly flattened out. These three amino acids are  
156 thus important for their contribution to the EMT-promoting effects of EntF\*, while the other  
157 amino acids contribute to a much lesser amount, as determined by the Fisher's LSD p-values

158 and confirmed using the Jenks natural break algorithm. Replacing the sixth amino acid of EntF\*  
159 by its unnatural D-amino acid isomer did also restore the E-cadherin expression to placebo  
160 levels. These results thus indicate that also the stereochemical configuration of the sixth amino  
161 acid of EntF\* is of importance for its EMT-promoting effects. Moreover, by using the  
162 antagonist Nef-M1 for the CXCR4 receptor, together with EntF\* on HCT-8 colorectal cells, the  
163 E-cadherin expression level increased from 62% to 94% (Cohen's d effect size of 1.2),  
164 indicating the interaction of EntF\* with the CXCL12 (or SDF-1)/CXCR4 pathway in tumour  
165 metastasis (*i.e.* EMT promotion). Interestingly, the modified peptide EntF\*1A, where the serine  
166 amino acid at position 1 of EntF\* is replaced by an alanine amino acid, could also be identified  
167 as having an antagonistic activity towards EntF\* on the CXCR4 receptor: E-cadherin  
168 expression levels increased from 62% to 92% (Cohen's d effect size of 0.8) when EntF\*1A was  
169 added to the EntF\*-treated cells (Fig. 2d).

170

171 ***In vivo pro-metastatic properties of EntF\* in mice***

172 Having demonstrated the presence of EntF\* *in vivo* as well as its *in vitro* effects, we  
173 evaluated its *in vivo* metastasis-promoting activities using an orthotopic colorectal cancer  
174 mouse model<sup>25,26</sup>. Before the luciferase-transfected HCT-8 cells were implanted into the wall  
175 of the caecum of the mice, cells were treated daily for five days with EntF\* (100 nM),  
176 phosphate-buffered saline (PBS) vehicle or Transforming Growth Factor  $\alpha$  (TGF $\alpha$ , positive  
177 control) (0.1  $\mu$ g mL $^{-1}$ ). On the sixth day, 6-weeks-old female Swiss nu/nu mice were  
178 orthotopically injected with the luciferase-transfected colorectal cancer cells, followed by a  
179 once-daily i.p. treatment of EntF\* (100 nmol kg $^{-1}$ ), PBS vehicle or Epidermal Growth Factor  
180 (EGF, positive control) (100  $\mu$ g kg $^{-1}$ ) (Fig. 3a). The *in vivo* distribution profile of EntF\* in these  
181 mice was then determined, after which the EntF\* daily exposure after i.p. treatment of 100 nmol  
182 kg $^{-1}$  was calculated. Additionally, the natural endogenous daily exposure was calculated from

183 the obtained endogenous EntF\* levels, described in supplementary Table 1. Based on both  
184 exposure calculations, it could be concluded that daily injections of 100 nmol kg<sup>-1</sup> EntF\* gave  
185 daily peptide exposures which were five times higher than the endogenous (natural) exposure  
186 in those mice, hence, in the range of the “positive” mice, thus demonstrating the biological  
187 relevance of this experimental set-up (Fig. 3b). Bioluminescent imaging of the mice was  
188 performed weekly to monitor the tumour growth (Fig. 3c). During the course of 6 weeks, EntF\*  
189 caused a statistically significant increase in luciferase activity compared to vehicle (p=0.030).  
190 This increase was even not significantly different from the well-established positive control  
191 EGF (p=0.319; Fig. 3d). Our results thereby demonstrated, after 6 weeks treatment, an effect  
192 size of 128% increase in bioluminescence for EntF\* compared to the placebo PBS, varying  
193 from -75%, a relative small negative association, to a 1494% increase, a substantial positive  
194 association (Fig. 4a). For the positive control EGF, a median effect size of 316% was obtained,  
195 ranging from -145% to 850%. This was confirmed by the number of tumour nodules counted  
196 macroscopically on the caecum, which was again statistically significantly higher with EntF\*  
197 in comparison to PBS (p=0.036) (Fig. 3d-e), demonstrating the *in vivo* 3-fold increase in the  
198 number of nodules due to this quorum sensing peptide metabolite while EGF showed a 4.5-fold  
199 increase (Fig. 4b).

200 Histopathological data further showed a significant higher number of tumours in both  
201 lungs and liver: a significantly higher number of tumour nodules was found in the liver  
202 (p=0.014) and lungs (p=0.026) after EntF\* treatment for 6 weeks, compared to vehicle  
203 treatment (Fig. 5a-d). This is important, as the liver is the most common site of metastases from  
204 colorectal cancer: in clinical practice, up to half of all patients with colorectal cancer will  
205 develop hepatic metastases, with a median survival of only 8 months and a 5-year survival of  
206 less than 5%<sup>26-30</sup>.

207 Another quorum sensing peptide (*i.e.* Phr0662 from *Bacillus* species), which also  
208 promoted *in vitro* cell invasion in our initial screening experiments<sup>13</sup>, showed no *in vivo*  
209 metastasis-promoting effects in the same orthotopic colorectal cancer mouse model  
210 (Supplementary Fig. 4). These findings indicate the selectivity of the quorum sensing peptides  
211 on the *in vivo* metastasis effects.

212 To evaluate the possible human relevance of our findings, the potential of *E. faecium* bacterial  
213 strains from human sources to produce EntF\* was investigated. Next to an initial BLAST  
214 search, bacterial strains, isolated from human faecal samples, were investigated at DNA level.  
215 The results showed that different EntF-containing *E. faecium* strains are present in different  
216 human faecal samples (Supplementary Tables 2 and 3), while on the other hand, also *E. faecium*  
217 strains without this EntF gene in their genome exist (Supplementary Table 2).

218

## 219 CONCLUSIONS

220 Collectively, our findings demonstrate that EntF\*, a microbiota-derived quorum sensing  
221 peptide metabolite, is present *in vivo* in biofluids of mice and promotes the metastasis of CRC  
222 in an orthotopic animal model, with a potency comparable to that of the well-established human  
223 colorectal cancer growth factor, EGF. Our findings are the first indication that quorum sensing  
224 peptides are an additional factor in microbiota-host interactions potentially influencing CRC  
225 metastasis. Our results offer new perspectives in research and development, ultimately offering  
226 new possibilities in disease prevention, diagnosis and therapy by selective modulation of the  
227 gut microbiome.

228

## 229 METHODS

### 230 Tissue homogenate preparation

231       Krebs-Henseleit (KH) buffer (pH 7.4) (Sigma-Aldrich, Belgium) was prepared by  
232       dissolving the powdered medium in 900 mL water while stirring. To this solution, 0.3790 g  
233       CaCl<sub>2</sub>×2H<sub>2</sub>O and 2.098 g NaHCO<sub>3</sub> are subsequently added while stirring. NaOH or HCl was  
234       used to adjust to pH 7.4. This solution was then further diluted to 1000 mL using ultrapure  
235       water.

236       For the preparation of colon tissue homogenate that was used for the EntF *in vitro*  
237       metabolization study, two colons were collected from two C57BL/6 female mice after cervical  
238       dislocation. The used mice received no treatment. After cleaning and rinsing the organs using  
239       ice-cold KH buffer, the colons were cut in little pieces and transferred into a 15 mL tube to  
240       which 5 mL ice-cold KH buffer was added. The colons were then homogenized for 1 minute.  
241       After the larger particles were allowed to settle for about 30 minutes at 5°C, approximately 2  
242       mL of the middle layer was dispensed into a 2 mL Eppendorf tube, and stored at -35°C until  
243       use. Just before use, the homogenate was diluted to a protein concentration of 0.6 mg/mL.

244       Faeces homogenate was prepared by collecting faeces from two non-treated C57BL/6  
245       female mice after cervical dislocation. The same procedures as with the colon tissue were  
246       performed. Just before use, the homogenate was diluted to a protein concentration of 0.6  
247       mg/mL.

248

## 249       **Peptide adsorption**

250       Due to adsorption of EntF\* to different kinds of plastic and glass material, all tubes and  
251       containers were coated before use with a BSA-based anti-adsorption solution<sup>24</sup>.

252

## 253       **Metabolization kinetics**

254       500 µL of tissue homogenate and 400 µL of KH buffer were mixed, together with 100  
255       µL of KH buffer (blank) or 1 mg/mL EntF peptide solution (test), all equilibrated and incubated

256 at 37°C. After 0, 5, 10, 30, 60, 120 and 180 minutes, 100 µL aliquots were taken and  
257 immediately mixed with 100 µL of 1% V/V trifluoroacetic acid solution in water, heated for 5  
258 min at 95°C, and cooled for 30 min in an ice-bath. After centrifugation at 16,000 g for 30 min  
259 at 5°C, supernatants were analysed by LC<sub>1</sub>-MS<sub>1</sub> for EntF\* quantification.

260

## 261 **Cell culture**

262 Caco-2 and luciferase transfected HCT-8/E11 cells were grown in DMEM medium  
263 supplied with 10% foetal bovine serum (FBS) and 1% penicillin-streptomycin (10,000 U/mL)  
264 solution. The cells were cultured in an incubator set at 37°C and 5% CO<sub>2</sub>. When confluent, cells  
265 were detached using 0.25% trypsin-EDTA.

266 *E. faecium* strains (LMG 20720, LMG 23236, LMG 15710 and ATCC 8459) were  
267 grown overnight at 37°C in BHI medium under aerobic conditions.

268

## 269 **Western Blot analyses**

270 1 x 10<sup>6</sup> HCT-8 cells were seeded in each well of a 6-well plate. 24 hours post-seeding,  
271 cells were treated with EntF\* and its synthesised alanine-derived analogues (100 nM) or  
272 placebo. For the antagonist study, 1 µM Nef-M1 and EntF\*A1 were mixed with EntF\* (500  
273 nM). After 24 hours, cells were detached from the surface and lysed with Thermo Scientific  
274 RIPA-buffer. The protein concentration was then determined using the modified Lowry protein  
275 assay kit, according to the manufacturer's instructions. All samples were diluted to the same  
276 concentration (*i.e.* 4 µg/µL) using water and diluted 1:1 using 2x Laemmli buffer. Next, the  
277 samples were boiled for 5 min at 95°C for denaturation, after which centrifugation for 5 min at  
278 16,000g was performed; the supernatant was then used for Western blot analyses. Therefore,  
279 proteins (20 µg) were separated using a Bio-Rad Any kD gel (SDS-PAGE) and transferred to a  
280 PVDF membrane. Before the membranes were incubated with antibodies, non-specific binding

281 sites were blocked using 5% skimmed milk solution (1 hour). Western blot was performed using  
282 an anti-E-cadherin (1/1000) antibody and incubated overnight at 4°C. Signal intensity was  
283 normalized against the total protein content in the lanes. Anti-rabbit-HRP antibody was used  
284 for detection (1/2000) (1 hour). Finally, the substrate (5 min) was added and the results were  
285 analyzed using the Bio-Rad ChemiDoc EZ imager and Image Lab software. TBS buffer with  
286 0.05% Tween 20 was used for washing between the different steps.

287

## 288 **Intestinal permeability**

289 Caco-2 cells were seeded on Transwell polycarbonate membrane filters (0.4  $\mu$ m pore  
290 size) (Corning, Germany) at a density of  $2.6 \times 10^5$  cells/cm<sup>2</sup> and the permeability study  
291 performed as described by Hubatsch *et al.*<sup>31</sup>. Cells were filled with Hank's Balanced Salt  
292 Solution (HBSS) and the TER values measured before and after the experiment. Peptide  
293 solution (1  $\mu$ M) was added to the apical chamber and 300  $\mu$ L aliquots taken after 30, 60, 90 and  
294 120 min of incubation. Samples were analysed using LC<sub>1</sub>-MS<sub>1</sub>. Linear curve fitting was used  
295 to calculate the apparent permeability coefficient (P<sub>app</sub>).

296

## 297 **Sample collection and preservation**

298 Mice (C57BL/6), possessing their natural microbiome (*i.e.* unmanipulated mice, without  
299 any peptide or bacterial administration), were euthanized by cervical dislocation and the blood  
300 collected. After standing for 30 min on ice, blood was centrifuged at 1,000 g for 10 min (room  
301 temperature). The supernatant (serum) was then transferred and stored at -35°C until use.

302 After defaecation, two droppings of faeces were immediately collected and put in liquid  
303 nitrogen for max. 1 h. The samples were then stored at -80°C until use.

304

## 305 **Sample preparation**

306        50  $\mu$ L of mice serum was mixed with 150  $\mu$ L of 0.5% formic acid in acetonitrile. After  
307        sonication for 5 min and vortexing for 5 sec, the mixture was heated for 30 sec at 100°C. The  
308        solution was again vortexed and centrifuged for 20 min at 20,000 g (4°C). The supernatant was  
309        then further purified using solid phase extraction (SPE) on HyperSep C<sub>18</sub> plates (Thermo Fisher  
310        Scientific, Belgium), which were previously conditioned with acetonitrile and equilibrated with  
311        75% acetonitrile in water, containing 0.375% formic acid. After loading 150  $\mu$ L of the samples,  
312        120  $\mu$ L eluent was collected and the organic solvents evaporated using nitrogen (1 L/min) for  
313        5 minutes. The resulting solutions were then further diluted with 30  $\mu$ L of BSA-based anti-  
314        adsorption solution, followed by LC-MS analysis.

315        Bacterial culture medium was centrifuged for 10 min at 2095 g and 4°C, after which the  
316        supernatant was filtered through a 0.20  $\mu$ m filter. For the purification of the culture medium,  
317        200  $\mu$ L of broth was loaded on an Oasis HLB  $\mu$ Elution plate (Waters, Belgium), previously  
318        conditioned and equilibrated with acetonitrile and water, respectively. EntF was then eluted  
319        from the column using 200  $\mu$ L of 70% methanol in water containing 2% of formic acid, and the  
320        organic solvents evaporated using nitrogen (1 L/min) for 4 minutes. The resulting solution was  
321        then further diluted with 150  $\mu$ L of acetonitrile containing 2% of formic acid, followed by LC<sub>2</sub>-  
322        MS<sub>1</sub> analysis.

323

#### 324        **RP-UPLC-TQ-MS (LC<sub>1</sub>-MS<sub>1</sub>) analysis**

325        EntF\* was detected and quantified on a Waters Acquity UPLC H-class system, connected  
326        to a Waters Xevo<sup>TM</sup> TQ-S triple quadrupole mass spectrometer with electrospray ionization  
327        (operated in positive ionization mode). Autosampler tray and column oven were thermostated  
328        at 10°C  $\pm$  5°C and 60°C  $\pm$  5°C, respectively. Chromatographic separation was achieved on a  
329        Waters Acquity<sup>®</sup> UPLC BEH Peptide C<sub>18</sub> column (300 Å, 1.7  $\mu$ m, 2.1 mm x 100 mm). The  
330        mobile phases consisted of 93:2:5 water:acetonitrile:DMSO (V/V) containing 0.1% formic acid

331 (i.e. mobile phase A) and 2:93:5 water:acetonitrile:DMSO (V/V) containing 0.1% formic acid  
332 (i.e. mobile phase B), and the flow rate was set to 0.5 mL/min. From the samples, a 10  $\mu$ L  
333 aliquot was injected. The gradient program started with 80% of mobile phase A for 1 minute,  
334 followed by a linear gradient to 40% of mobile phase A for 3.5 minutes. Gradient was then  
335 changed to 14.2% mobile phase A at 5 min, followed by a 1 min equilibration, before starting  
336 conditions were applied. EntF\* showed retention at 4.25 – 4.45 min.

337 An optimised capillary voltage of 3.00 kV, a cone voltage of 20.00 V and a source offset  
338 of 50.0 V was used. Acquisition was done in the multiple reaction monitoring (MRM) mode.  
339 The selected precursor ion for EntF\* was  $m/z$  865.7 with two selected product ions at  $m/z$  202.08  
340 (36 eV, b<sub>2</sub> fragment) as quantifier and  $m/z$  315.17 (31 eV, b<sub>3</sub> fragment) as qualifier.

341 A sample was considered positive for the presence of EntF\* when following criteria were  
342 met: correct retention time, quantifier/qualifier peak area ratio's between 2.0 and 4.0, both  
343 quantifier and qualifier with a signal-to-noise ratio above 3.0 and a concentration above the  
344 LOQ of 100 pM.

345

#### 346 **RP-UPLC-QTOF-MS (LC<sub>1</sub>-MS<sub>2</sub>) analysis**

347 Chromatographic separation was achieved on a Waters Acquity® UPLC HSS T3  
348 Column (100  $\text{\AA}$ , 1.8  $\mu$ m, 2.1 mm x 100 mm), with detection using the Waters SYNAPT G2-Si  
349 High Definition Mass Spectrometry with electrospray ionization (operated in the positive  
350 ionization mode). Gradient composition and UPLC-MS settings were the same as with the LC<sub>1</sub>-  
351 MS<sub>1</sub> method; a TOF-MS/MS mode was applied with a fixed mass on the quadrupole of 865.157,  
352 a fixed trap collision energy of 30 eV and an acquired MS/MS over the range of 100-1450 m/z  
353 (scan time 1 second). EntF\* retention was observed between 3.40-3.50 min. When at least four  
354 daughter ions ( $m/z \pm 0.05$ ) of EntF\* were detected at the expected retention time and at least

355 three of the most abundant isotope parent peaks ( $m/z \pm 0.05$ ) were detected, the sample was  
356 considered to contain the EntF\* peptide.

357

### 358 **RP-UPLC-QOrbitrap-MS (LC<sub>1</sub>-MS<sub>3</sub>) analysis**

359 While the UPLC separation system was the same as with the LC<sub>1</sub>-MS<sub>1</sub> method, the third  
360 detection system consisted of a Thermo Fisher Q Exactive™ Hybrid Quadrupole-Orbitrap Mass  
361 Spectrometer. The mass spectrometer was operated using a heated electrospray ionization  
362 source with the following setting: capillary temperature set at 300°C, S-Lens RF level set at 50,  
363 spray voltage set at 3.00 kV and auxiliary gas flow set at 20.

364 A full MS/MS mode was applied with a fixed mass on the quadrupole of 865.157, a fixed  
365 trap collision energy of 30 eV and 35 eV and an acquired MS/MS over the range of 100-1800  
366  $m/z$ . EntF\* retention was observed at 4.13-4.16 min. When at least two daughter ions ( $m/z \pm$   
367 0.005) of EntF\* were detected at the expected retention time and at least four of the most  
368 abundant isotope parent peaks ( $m/z \pm 0.005$ ) were detected, the sample was considered to be  
369 positive for the presence of EntF\*.

370

### 371 **HILIC-UPLC-TQ-MS (LC<sub>2</sub>-MS<sub>1</sub>) analysis**

372 Chromatographic separation was achieved on a Waters Acquity® UPLC BEH Amide  
373 Column (130 Å, 1.7 µm, 2.1 mm x 100 mm). Mobile phase composition, sample volume, flow  
374 rate and MS settings were the same as described for the LC<sub>1</sub>-MS<sub>1</sub> method. For EntF\*  
375 quantification in mouse serum, the gradient program started with 10% of mobile phase A for 2  
376 minutes, followed by a linear gradient to 40% of mobile phase A for 3.0 minutes. Gradient was  
377 then changed to 85% mobile phase A at 6 min, followed by a 1 min equilibration, before starting  
378 conditions were applied. EntF\* showed retention at 4.85 – 4.95 min. A sample was considered  
379 positive for the presence of EntF\* when following criteria were met: correct retention time,

380 both daughter fragments (*i.e.* b<sub>2</sub> (quantifier) and b<sub>3</sub> (qualifier) fragment ions) with a signal-to-  
381 noise ratio above 3.0 and quantifier/qualifier peak area ratio's between 2.0 and 4.0.

382 For the quantification of EntF in culture medium, the gradient program started with 100%  
383 of mobile phase B for 2 minutes, followed by a linear gradient to 40% of mobile phase B for 7  
384 minutes, cleaning at 85% B and re-equilibration at starting conditions. Acquisition was done in  
385 the multiple reaction monitoring (MRM) mode. The selected precursor ion for EntF was *m/z*  
386 667.1 with three selected product ions: *m/z* 129.0 (30 eV, b<sub>2</sub> fragment) and *m/z* 662.6 (22 eV,  
387 b<sub>25</sub> fragment), both as qualifier, and *m/z* 949.4 (22 eV, y<sub>17</sub> fragment) as quantifier.

388

### 389 **DNA extraction of faeces**

390 To 20-40 mg faeces, 500 mg of unwashed glass beads, 0.5 mL CTAB buffer  
391 (hexadecyltrimethylammonium bromide 5% (w/v), 0.35 M NaCl, 120 mM K<sub>2</sub>HPO<sub>4</sub>) and  
392 0.5 mL phenol-chloroform-isoamyl alcohol mixture (25:24:1) were added. The mixture was  
393 homogenized two times for 1.5 min at 22.5 Hz using a TissueLyser II (Qiagen, Belgium). The  
394 mixture was centrifuged for 10 minutes at 8,000 rpm and 300 µL of the supernatant was  
395 transferred to a new Eppendorf tube. For a second time, 0.25 mL of CTAB buffer was added to  
396 the original DNA sample, which was again homogenized in the TissueLyser and centrifuged  
397 for 10 minutes at 8,000 rpm. Of this supernatant, 300 µL was added to the first 300 µL  
398 supernatant. The phenol was removed by adding an equal volume of chloroform-isoamyl  
399 alcohol (24:1) followed by centrifugation at 16,000 g for 10 sec. The aqueous phase was  
400 transferred to a new tube. Nucleic acids were precipitated with 2 volumes PEG-6000 solution  
401 (polyethyleenglycol 30% (w/v), 1.6 M NaCl) for 2 h at room temperature. The pellet was  
402 obtained by centrifugation at 13,000 g for 20 min and washed with 1 mL of ice-cold 70% (v/v)  
403 ethanol. After centrifugation at 13,000 g for 20 min, the pellet was dried and resuspended in 50

404  $\mu$ L de-ionized water. The quality and the concentration of the DNA was examined  
405 spectrophotometrically.

406

#### 407 **qPCR on faeces**

408 qPCR was performed using SYBR-green 2x master mix in a Bio-Rad CFX-384 system.  
409 Each reaction was done in sixfold in a 12  $\mu$ L total reaction mixture using 2  $\mu$ L of the DNA  
410 sample and 0.5  $\mu$ M final qPCR primer concentration. The qPCR conditions used: 1 cycle of  
411 95°C for 10 min, followed by 40 cycles of 95°C for 30 sec, 60°C for 30 sec, and stepwise  
412 increase of the temperature from 65° to 95°C (at 10 sec/0.5°C). Melting curve data were  
413 analysed to confirm the specificity of the reaction. Samples with aspecific melting peaks were  
414 discarded from further analyses. The copy numbers of samples were determined by comparison  
415 of their Ct values to the standard curve. For the creation of the standard curves, the PCR product  
416 was generated using the standard fragment PCR primers, listed in Supplementary Figure 2, and  
417 DNA from *E. faecium* strain 100-1. After purification (MSB Spin PCRapace, Stratec Molecular,  
418 Berlin, Germany) and determination of the DNA concentration, the concentration of the linear  
419 dsDNA standard was adjusted to  $1 \times 10^7$  to  $1 \times 10^1$  copies per  $\mu$ L with each step differing by 10-  
420 fold. Because the Cq values of the EntF\* qPCR analyses were around the limit of detection  
421 (LOD), with a notable amount of left-truncated data (data below LOD), a maximum likelihood  
422 (ML) approach was used to find the best estimation of mean and standard deviation for each  
423 sample.

424

#### 425 **Standard protein BLAST**

426 The amino acid sequence of the EntF\* peptide was blasted against the NCBI non-  
427 redundant (nr) database by Basic Local Alignment Search Tool protein (BLASTp). This blast

428 search was performed with the organism limited to bacteria (taxid:2). Only alignment hits with  
429 a 100% coverage and 100% identity were retained.

430

431 **Orthotopic colorectal cancer mouse model**

432 All *in vivo* experiments were performed according to the Ethical Committee principles of  
433 laboratory animal welfare and approved by our institute (Ghent University, Faculty of Medicine  
434 and Health Sciences, approval number ECD 17-90). Mice were maintained in a sterile  
435 environment with light, humidity and temperature control (light–dark cycle with light from  
436 7:00 h to 17:00 h, temperature 21–25°C and humidity 45–65%). Before the experiment, mice  
437 were allowed to acclimatize for a minimum of seven days.

438 Six-weeks old female athymic nude mice (Swiss nu/nu) were anesthetized and a small  
439 midline laparotomy executed to localize the caecum. The caecum was then gently exteriorized  
440 and luciferase transfected HCT-8/E11 cells ( $1 \times 10^6$  cells) in a volume of 20 µL serum-free  
441 DMEM medium with matrigel (1:1) injected into the caecal wall. Cells were previously treated  
442 with EntF\* (10 nM, 100 nM or 1 µM), Phr0662 (100 nM) or with the vehicle (PBS) or positive  
443 control (Transforming Growth Factor  $\alpha$  (TGF $\alpha$ ), 0.1 µg mL $^{-1}$ ) solution for 5 days before they  
444 were implanted in the mice. The caecum was then carefully returned to the abdominal cavity  
445 and the laparotomy closed in two layers by sutures of PDS 6/0. Starting from the day after  
446 tumour cell injection, mice were daily treated with vehicle (PBS, n = 15), EntF\* (10 nmol kg $^{-1}$ ,  
447 n = 12; 100 nmol kg $^{-1}$ , n = 18; 1 µmol kg $^{-1}$ , n = 8), Phr0662 (100 nmol kg $^{-1}$ , n = 5) or positive  
448 control (Epidermal Growth Factor (EGF), 100 µg kg $^{-1}$ , n = 18) for 6 weeks. Once a week, mice  
449 were investigated for tumour growth and metastases using bioluminescent imaging with the  
450 IVIS Lumina II (Perkin Elmer, Belgium) after i.p. injection with 200 µL luciferin (150 mg kg $^{-1}$ ,  
451). After 6 weeks, mice were euthanized using cervical dislocation, followed by macroscopic  
452 evaluation of the liver, diaphragm, lungs, caecum, duodenum and peritoneum for the presence

453 of tumour nodules. Liver and lung tissues were then fixed in formalin during 24 h and stored in  
454 70% ethanol for max. 3 days before embedding in paraffin. Afterwards, a haematoxylin & eosin  
455 (H&E) staining was performed on 8  $\mu$ m sections and 3 sections were visualized per mouse  
456 using microscopy. The slides of all tumour-bearing mice were scored by two blinded,  
457 independent investigators using a scoring system as described in Supplementary Table 4. In the  
458 case of a difference in scoring, the slide was scored again by a third blinded, independent  
459 investigator for consensus.

460 Daily peptide exposures were calculated after i.p. injection of 25  $\mu$ L of a 100  $\mu$ M EntF\*  
461 solution into female Swiss nu/nu mice (n=14), followed by LC<sub>1</sub>-MS<sub>1</sub> analyses of mice serum  
462 at different time points after injection. A distribution and early exponential phase ( $\alpha$ , 0-30 min),  
463 followed by a terminal elimination phase ( $\beta$ , 30-180 min) could be distinguished. The exposure  
464 was determined for 24 hours (x) as follows: *Exposure (nM x min) =  $\int_0^{30} A e^{-\alpha t} + \int_{30}^x B e^{-\beta t}$* .

465

#### 466 **PCR on *E. faecium* strains**

467 *E. faecium* was grown in BHI medium. DNA was extracted using alkaline lysis after  
468 which the EntF\* fragment was amplified using 2x Biomix (Bioline, Belgium) in a Mastercycler  
469 PCR system (Eppendorf, Belgium). Each reaction was performed in a 10  $\mu$ L total reaction  
470 mixture using 1  $\mu$ L of the DNA sample and 0.5  $\mu$ M final primer concentration (EntF\*-PCR  
471 primers, Supplementary Fig. 2). The PCR conditions used: 1 cycle of 94°C for 5 min, followed  
472 by 30 cycles of 94°C for 30 sec, 55°C for 30 sec and 72°C for 1 min. Final elongation was  
473 performed at 72°C for 10 min, after which the PCR product was held at 4°C. The PCR  
474 amplification products were visualized on 1.5% agarose gel.

475

#### 476 **Statistical analyses**

477 A quantitative approach was used to evaluate the importance of each amino acid, where  
478 the Fisher's LSD p-values of (1) the multiple comparison between EntF\* and the alanine scan  
479 and (2) the multiple comparison between different peptides of the alanine scan are combined.  
480 Subsequently, based on the combined P-score, the amino acids were classified in 5 classes using  
481 a hierarchical cluster analysis, and confirmed using the Jenks natural break algorithm with  
482 K=5.

483 The Kolmogorov-Smirnov test was used to assess if data obtained were normally  
484 distributed. For sample sizes of  $n < 10$ , non-parametric tests (Mann-Whitney U test) were  
485 performed directly. Slope comparison was based on linear regression analysis. Bootstrapped  
486 medians and Hedges G-values were used to calculate the effect size when sample sizes were  
487 different between the groups. Cohen's d values were calculated as a measure of the effect size  
488 when similar standard deviations for both groups were found and sample sizes were the same.

489

490

491 **DECLARATIONS**

492 **Ethics approval and consent to participate**

493 Not applicable.

494 **Consent for publication**

495 Not applicable.

496 **Availability of data and material**

497 Not applicable.

498 **Competing interests**

499 The authors declare no competing interests.

500 **Funding**

501 This work was supported by the Research Foundation Flanders (1S21017N to ND and  
502 1158818N to ADS) and by the Institute for the Promotion of Innovation through Science and  
503 Technology in Flanders (131356 to FV).

504 **Author contributions**

505 N.D. and E.W. performed the experiments, with a major contribution on the LC-MS analyses  
506 and *in vivo* mice studies. Y.J. and F.V. helped with the Western Blot analyses; A.D.S. and L.T.  
507 helped with the qPCR analyses and *in vivo* mice studies, respectively. N.D., Y.J., S.V.W., D.L.  
508 and B.D.S designed the Western Blot experiments and discussed the results. N.D., E.W.,  
509 A.D.S., E.G., F.V.I. and B.D.S. designed the qPCR analyses and evaluated the data. N.D., D.K.  
510 and R.H. performed the peptide synthesis of the alanine-derived peptide analogues. E.W.,  
511 C.V.D.W., O.D.W. and B.D.S. designed the *in vivo* mice studies. N.D., E.W. and B.D.S. wrote  
512 the manuscript with input from all co-authors.

513 **Acknowledgements**

514 We thank the group of Ward De Spieghelaere and Wim Van Den Broeck for helping with the  
515 paraffin processing of the tissues.

516

517

518 **REFERENCES**

519 [1] S. Kopetz, New therapies and insights into the changing landscape of colorectal cancer.  
520 Nature Reviews Gastroenterology & Hepatology 2019;16:79-80.

521 [2] R.C. Bates, A.M. Mercurio, The epithelial-mesenchymal transition (EMT) and colorectal  
522 cancer progression. Cancer Biology and Therapy 2005;4:365-70.

523 [3] D. Gingras, R. Bélineau, Colorectal cancer prevention through dietary and lifestyle  
524 modifications. Cancer Microenvironment 2011;4:133-9.

525 [4] S.I. Grivennikov, Inflammation and colorectal cancer: colitis-associated neoplasia.  
526 Seminars in Immunopathology 2013;35:229-44.

527 [5] Q. Feng, S. Liang, H. Jia, A. Stadlmayr, L. Tang et al., Gut microbiome development along  
528 the colorectal adenoma-carcinoma sequence. Nature Communications 2015;6:6528.

529 [6] P. Louis, G.L. Hold, H.J. Flint, The gut Microbiota, bacterial metabolites and colorectal  
530 cancer. Nature Reviews Microbiology 2014;12:661-72.

531 [7] Y. Janssens, J. Nielandt, A. Bronselaer, N. Debuinne, F. Verbeke et al., Disbiome database:  
532 linking the microbiome to disease. BMC Microbiology 2018;50:1-6.

533 [8] Y. Lu, J. Chen, J. Zheng, G. Hu, J. Wang et al., Mucosal adherent bacterial dysbiosis in  
534 patients with colorectal adenomas. Scientific reports 2016;6:26337.

535 [9] T. Wang, G. Cai, Y. Qiu, N. Fei, M. Zhang et al., Structural segregation of gut microbiota  
536 between colorectal cancer patients and healthy volunteers. The ISME Journal 2012;6:320-29.

537 [10] S. Kang, S.E. Denman, M. Morrison, Z. Yu, J. Dore et al., Dysbiosis of fecal microbiota  
538 in Crohn's disease patients as revealed by a custom phylogenetic microarray. Inflammatory  
539 Bowel Diseases 2010;16:2034-42.

540 [11] V. Pascal, M. Pozuela, N. Borruel, F. Casellas, D. Campos et al., A microbial signature for  
541 Crohn's disease. Gut 2017;66:813-22.

542 [12] J. Ni, G.D. Wu, L. Albenberg, V.T. Tomov, Gut microbiota and IBD: causation or  
543 correlation? Nature reviews Gastroenterology & Hepatology 2017;14:573-84.

544 [13] E. Wynendaele, F. Verbeke, M. D'Hondt, A. Hendrix, C. Van De Wiele et al., Crosstalk  
545 between the microbiome and cancer cells by quorum sensing peptides. Peptides 2015;64:40-8

546 [14] B. De Spiegeleer, F. Verbeke, M. D'Hondt, A. Hendrix, C. Van De Wiele et al., The  
547 quorum sensing peptides PhrG, CSP and EDF promote angiogenesis and invasion of breast  
548 cancer cells in vitro. PloS one 2015;10:e0119471.

549 [15] Y. Janssens, E. Wynendaele, F. Verbeke, N. Debuinne, B. Gevaert et al., Screening of  
550 quorum sensing peptides for biological effects in neuronal cells. Peptides 2018;101:150-6.

551 [16] A. De Spiegeleer, D. Elewaut, N. Van Den Noortgate, Y. Janssens, N. Debrunne et al.,  
552 Quorum sensing molecules as a novel microbial factor impacting muscle cells. *Biochimica et*  
553 *biophysica acta. Molecular basis of disease* 2020;1866;165646.

554 [17] E. Wynendaele, A. Bronselaer, J. Nielandt, M. D'Hondt, S. Stalmans et al., Quorumpeps  
555 database: chemical space, microbial origin and functionality of quorum sensing peptides.  
556 *Nucleic Acids Research* 2013;41:655-9.

557 [18] M.J. van Belkum, D.J. Derkens, C.M. Franz, J.C. Vedera, Structure function relationship  
558 of inducer peptide pheromones involved in bacteriocin production in *Carnobacterium*  
559 *maltaromaticum* and *Enterococcus faecium*. *Microbiology* 2007;153:3660-6.

560 [19] C.M. Franz, M.J. van Belkum, R.W. Worobo, J.C. Vedera, M.E. Stiles, Characterization  
561 of the genetic locus responsible for production and immunity of carnobacteriocin A: the  
562 immunity gene confers cross-protection to enterocin B. *Microbiology* 2000;146:621-31.

563 [20] T. Nilsen, I.F. Nes, H. Holo, An exported inducer peptide regulates bacteriocin production  
564 in *Enterococcus faecium* CTC492. *Journal of Bacteriology* 1998;180:1848-54.

565 [21] T. Aymerich, H. Holo, L.S. Havarstein, M. Hugas, M. Garriga et al., Biochemical and  
566 genetic characterization of enterocin A from *Enterococcus faecium*, a new antilisterial  
567 bacteriocin in the pediocin family of bacteriocins. *Applied and Environmental Microbiology*  
568 1996;62:1676-82.

569 [22] K. Dubin, E.G. Pamer. Enterococci and Their Interactions with the Intestinal Microbiome.  
570 *Microbiol Spectr.* 2014;5:10.

571 [23] C. Darkoh, H.L. DuPont, S.J. Norris, H.B. Kaplan, Toxin synthesis by *Clostridium*  
572 *difficile* is regulated through quorum signaling. *mBio* 2015;6:e02569.

573 [24] F. Verbeke, N. Bracke, N. Debrunne, E. Wynendaele, B. De Spiegeleer, LC-MS  
574 Compatible Antiadsorption Diluent for Peptide Analysis. *Analytical chemistry* 2020; 92: 1712-  
575 19.

576 [25] A. Fumagalli, S.J.E. Suijkerbuijk, H. Begthel, E. Beerling, K.C. Oost et al., A surgical  
577 orthotopic organoid transplantation approach in mice to visualize and study colorectal cancer  
578 progression. *Nature protocols* 2018;13:235-47.

579 [26] M.D. Smith, J.L. McCall. Systematic review of tumour number and outcome after radical  
580 treatment of colorectal liver metastases. *Br. J. Surg.* 2009;96:1101-19.

581 [27] L.H. Xu, S.J. Cai, G.X. Cai, W.J. Peng, Imaging diagnosis of colorectal liver metastases.  
582 *World J. Gastroenterol.* 2011;17:4654-59.

583 [28] K.T. Nguyen, A. Laurent, I. Dagher, D.A. Geller, J. Steel et al., Minimally invasive liver  
584 resection for metastatic colorectal cancer: a multi-institutional, international report of safety,  
585 feasibility, and early outcomes. *Ann. Surg.* 2009;250:842-48.

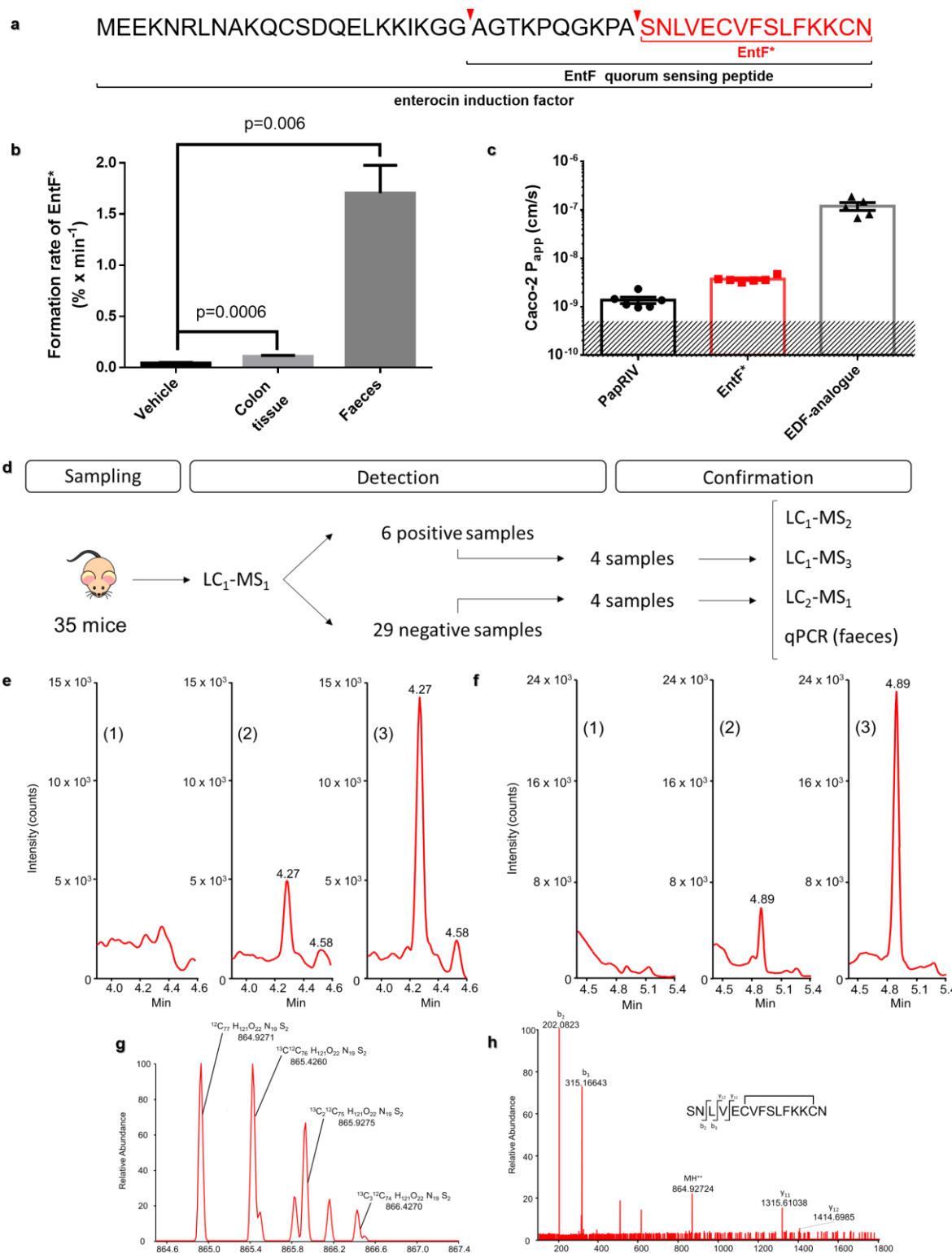
586 [29] J.W. Holch, M. Demmer, C. Lamersdorf, M. Michl, C. Schulz et al., Pattern and dynamics  
587 of distant metastases in metastatic colorectal cancer. *Visceral Medicine* 2017;33:70-5.

588 [30] J. Tommelein, E. De Vlieghere, L. Verset, E. Melsens, J. Leenders et al., Radiotherapy-  
589 activated cancer-associated fibroblasts promote tumor progression through paracrine IGF1R  
590 activation. *Cancer Research* 2018;79:659-70.

591 [31] I. Hubatsch, E.G.E. Ragnarsson, P. Artursson, Determination of drug permeability and  
592 prediction of drug absorption in Caco-2 monolayers. *Nature Protocols* 2007;2:2111-9.

593

594 **FIGURES**

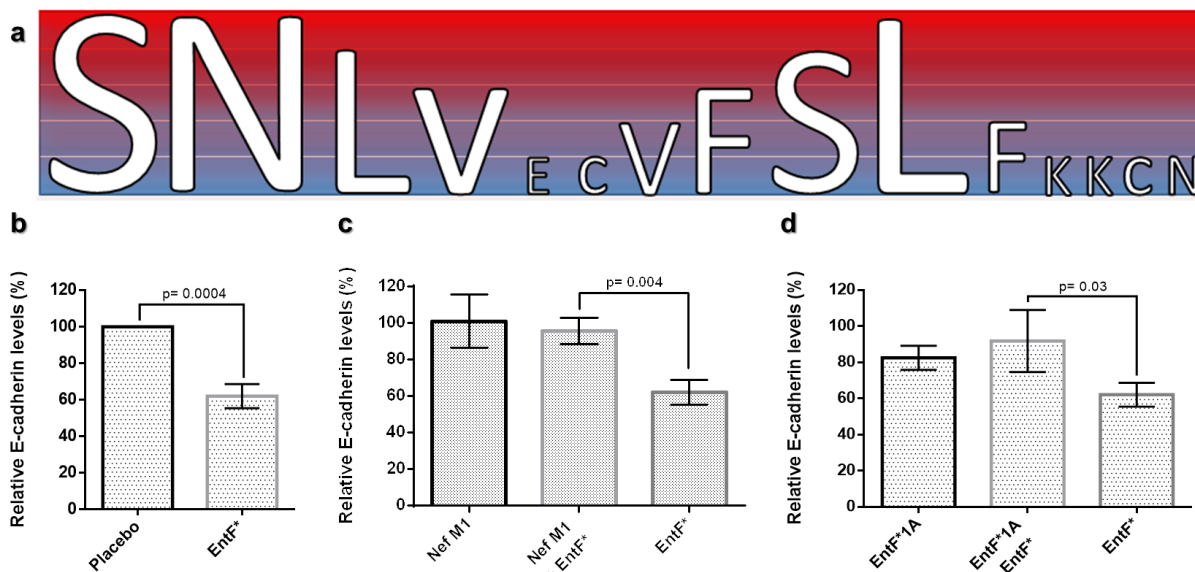


595

596 **Figure 1: *In vitro* formation and *in vivo* presence of the EntF quorum sensing peptide-derived metabolite. a, Sequence of the quorum sensing propeptide enterocin induction factor, 597 the mature quorum sensing peptide EntF and its metabolite EntF\*. b, The *in vitro* formation 598**

599 rate of EntF\* from EntF in colon and faeces homogenate. Bars represent mean formation rate  
600  $\pm$  s.e.m from 6 (colon), resp. 4 (faeces) independent experiments. Statistically significant  
601 differences were determined by a Mann-Whitney U test with indicated p-values. **c**, CaCo-2  
602 apparent permeability coefficients ( $P_{app}$ ) of 3 different quorum sensing peptides. Bars represent  
603 mean  $P_{app}$ -values  $\pm$  s.e.m. (n=5-6 independent experiments per group); the shaded area  
604 represents the limit of detection. **d**, Flow chart of *in vivo* data acquisition, from sampling of  
605 serum samples to detection and confirmation of EntF\*. Different LC-MS methods: reversed-  
606 phase ultra-high-performance liquid chromatography (RP-UPLC) using triple quadrupole (TQ)  
607 in MRM mode (LC<sub>1</sub>-MS<sub>1</sub>), high-resolution quadrupole time-of-flight (LC<sub>1</sub>-MS<sub>2</sub>), high-  
608 resolution quadrupole-orbitrap (LC<sub>1</sub>-MS<sub>3</sub>) and HILIC-amide UPLC using TQ in MRM mode  
609 (LC<sub>2</sub>-MS<sub>1</sub>). qPCR was performed on faeces samples from those mice to demonstrate the  
610 presence of EntF\*-containing *E. faecium* DNA copies. **e**, Chromatographic profile of (1)  
611 negative serum sample; (2) positive serum sample; (3) serum of mice i.p. injected with EntF\*;  
612 all using RP-UPLC with detection by electrospray ionization mass spectrometry (ESI-MS)  
613 using TQ in MRM mode ( $m/z = 865 \rightarrow 202.08 + 315.17$ ). **f**, Chromatographic profile of (1)  
614 negative serum sample; (2) positive serum sample; (3) serum of mice i.p. injected with EntF\*;  
615 all using HILIC amide UPLC with detection by ESI-MS using TQ in MRM mode ( $m/z = 865$   
616  $\rightarrow 202.08 + 315.17$ ). **g**, Isotopic distribution of the double charged EntF\* measured in a positive  
617 serum sample using RP-UPLC with detection by ESI-MS using quadrupole-orbitrap. **h**, High-  
618 resolution tandem mass spectrum of EntF\* with characteristic fragments, using RP-UPLC with  
619 detection by Q-TOF.

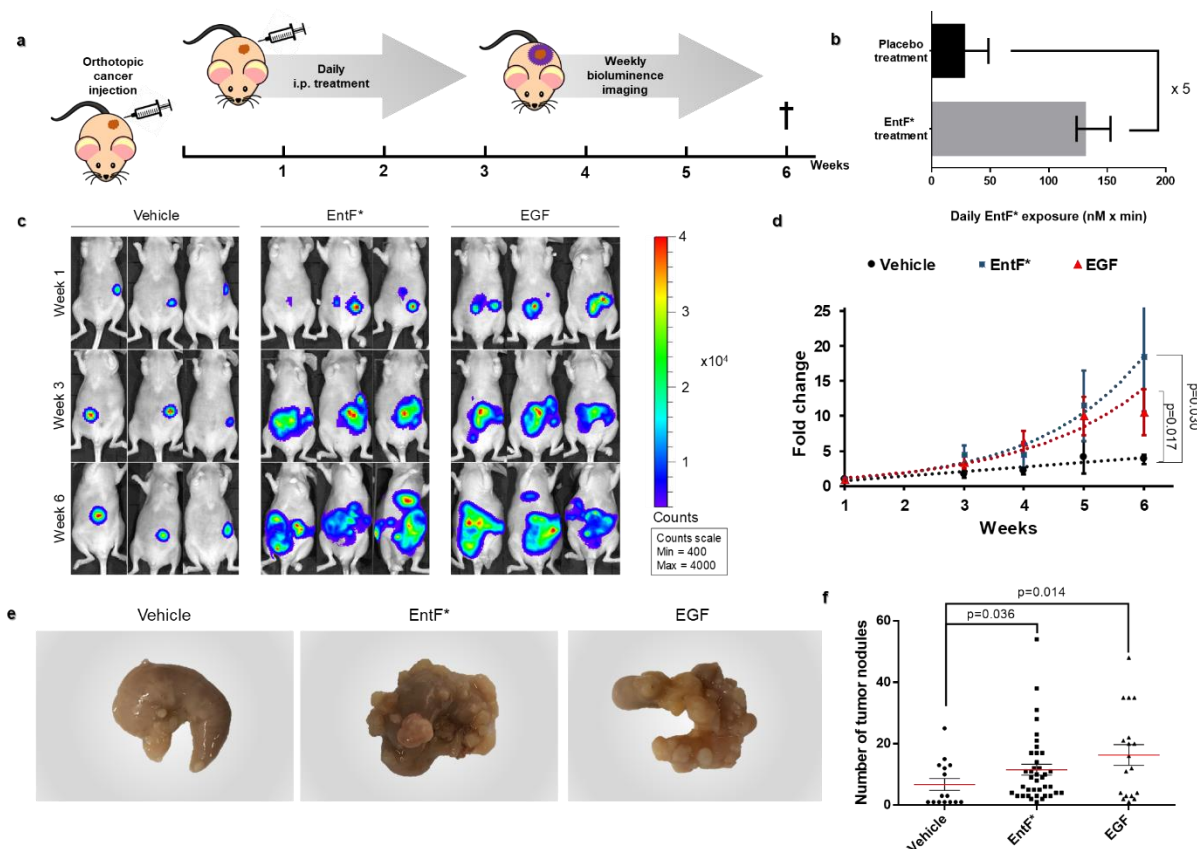
620



621

622 **Figure 2: *In vitro* activity of the EntF\* peptide. a,** Effect of alanine-derived EntF\* analogues  
623 on E-cadherin expression. Ranking in five classes (blue to red: increasing significance) was  
624 performed using the Fisher's LSD p-values, which was confirmed using the Jenks natural break  
625 algorithm. Based on ranking, it was proven that the first, second and tenth amino acid of EntF\*  
626 are the most important amino acids for the epithelial-mesenchymal promoting (EMT) effects  
627 of EntF\*. **b,** Effect of EntF\* on E-cadherin expression. A significant mean decrease of 38% in  
628 E-cadherin level for EntF\* in comparison with placebo was observed (one-way ANOVA,  
629 Fisher's LSD). **c,** The antagonistic effects of Nef-M1 on the E-cadherin reducing effect of EntF\*  
630 on HCT-8 cells. Statistically significant differences were determined by a one-sided student's t  
631 test. **d,** The antagonistic effects of EntF\*1A on the E-cadherin reducing effect of EntF\* on  
632 HCT-8 cells. Statistically significant differences were determined by a one-sided student's t test.

633

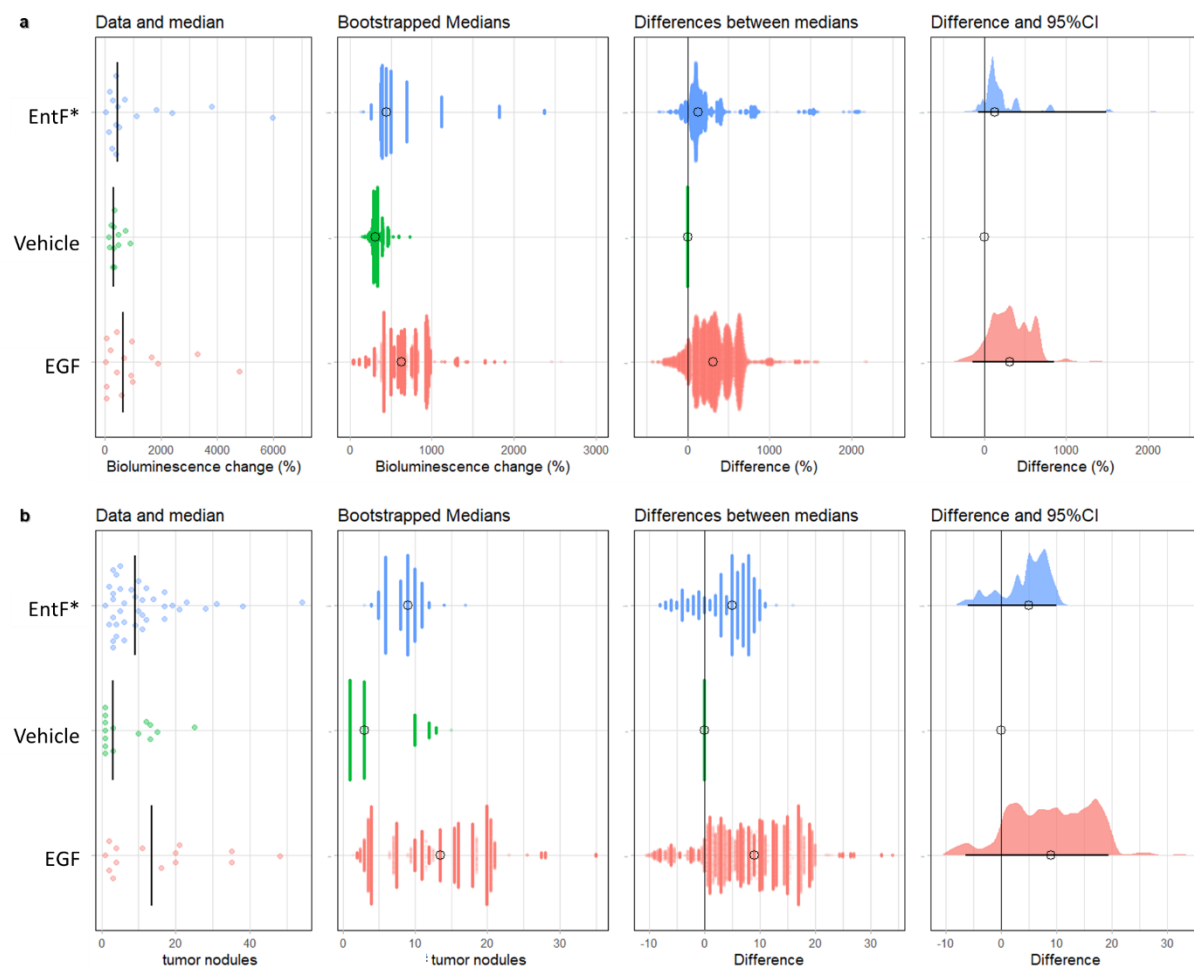


634

635 **Figure 3: In vivo metastasis-inducing effect of EntF\* in an orthotopic colorectal cancer**  
 636 **mouse model. a**, Experimental schematic timeline. Female Swiss nu/nu mice were  
 637 orthotopically injected with  $1 \times 10^6$  luciferase transfected HCT-8 cells at the age of 5 weeks.  
 638 During 6 weeks, the mice were daily i.p. injected with  $100 \text{ nmol kg}^{-1}$  EntF\*, PBS control or  $0.1$   
 639  $\text{mg kg}^{-1}$  EGF positive control. Bioluminescent imaging was performed weekly to determine  
 640 cancer progression. After 6 weeks, the mice were euthanized and the caecum, liver and lungs  
 641 collected. **b**, The daily exposure in the female Swiss nu/nu mice ( $n=65$  placebo mice, with  
 642 negative mice ( $< \text{LoQ} = 100 \text{ pM}$ ) set as  $0 \text{ pM}$ ) and the female Swiss nu/nu mice after  
 643 injection with EntF\* ( $n=14$ ) is given. Error bars represent s.e.m. values. It could be  
 644 concluded that the daily exposure after i.p. injection of  $100 \text{ nmol kg}^{-1}$  EntF\* (used for the  
 645 orthotopic colorectal cancer mouse model) is 5 times higher than the natural occurring EntF\*  
 646 levels. **c**, A representative image comparing the basal bioluminescence activity between the  
 647 three treatments. Mice were i.p. injected with  $150 \text{ mg kg}^{-1}$  luciferine and imaged 10 minutes  
 648 later in the supine position. **d**, Tumour growth curves of the three groups. Based on linear  
 649 regression slope comparison, the EntF\* as well as the positive control EGF treatment resulted  
 650 in a significant increase of tumour growth compared to the vehicle control with indicated p-  
 651 values. Data represent mean fold change  $\pm$  s.e.m. ( $n=17-18$  mouse per group). **e**, Macroscopic,

652 representative caecum pictures of the three treatments at the end of the experiment. **f**, Caecum  
653 tumour nodules were counted and the data represent the mean  $\pm$  s.e.m. Statistically significant  
654 differences were determined by a Mann-Whitney U test (n= 15-38 per group) with indicated p-  
655 values.

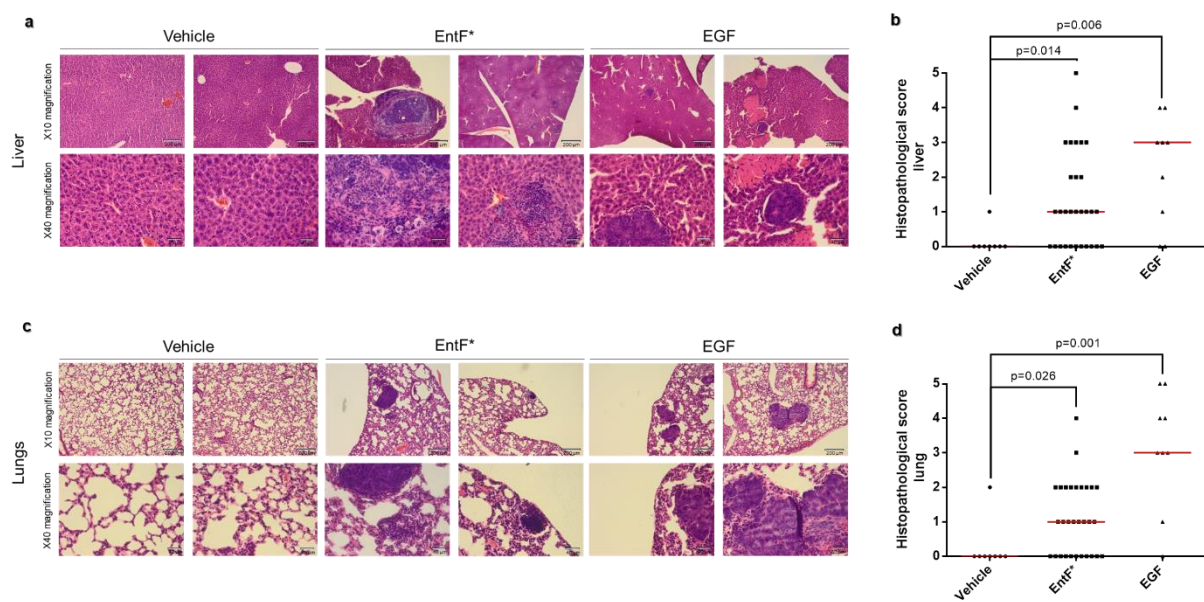
656



657

658 **Figure 4: Effect size for bioluminescence and the number of nodules on the caecum in the**  
659 **orthotopic mouse model after 6 weeks treatment. a,** After 6 weeks treatment, an effect size  
660 of 128% increase in bioluminescence for EntF\* compared to the placebo PBS was observed,  
661 while for the positive control EGF, a median effect size of 316% was obtained. When  
662 calculating the effect size according to Hedges' G values, a median to high effect was observed  
663 for both the EntF\* and the EGF treatment groups, compared to the placebo group. **b,** After 6  
664 weeks treatment, a 3-fold increase in the number of nodules on the caecum was observed for  
665 EntF\* compared to the placebo PBS, while for the positive control EGF, a 4.5-fold increase  
666 was obtained. When calculating the effect size according to Hedges' G values, a median and  
667 high effect was observed for the EntF\* and EGF treatment groups, respectively, compared to  
668 the placebo group.

669 [Figure prepared in R-script: <https://github.com/JoachimGoedhart/PlotsOfDifferences>]



670  
671 **Figure 5: Histopathological evaluation of CRC metastasis after EntF\* treatment. a,**  
672 Haematoxylin and eosin (H&E) staining of the liver with magnified images (x10 and x40). **b,**  
673 Histopathological scores with statistically significant differences determined by a Mann-  
674 Whitney U test ( $n= 8$  for PBS,  $n= 30$  for EntF\*,  $n= 9$  for EGF) with indicated p-values. **c,** H&E  
675 staining of the lungs with magnified images (x10 and x40). **d,** Histopathological scores with  
676 statistically significant differences determined by a Mann-Whitney U test ( $n= 8$  for PBS,  $n=$   
677 30 for EntF\*,  $n= 9$  for EGF) with indicated p-values.